A Model for Optoelectronically Interconnected Smart Pixel Arrays

Mohammad Azadeh, Robert B. Darling, *Senior Member, IEEE, Member, OSA*, and W. Randall Babbitt, Member, OSA

***Abstract*—Theoretical results for modeling source-based smart pixel arrays are presented. Attention is focused on modeling the nonlinearities in sources, as well as electrical and optical couplings and interactions within a single pixel. A matrix formalism is used to generalize the theory to include the behavior of an entire smart pixel array consisting of interacting pixels with arbitrary optical and electrical interconnections. A vertical cavity surface emitting laser (VCSEL)-based smart pixel array is used for experimental demonstration of the application of the theory in the design and implementation of an optoelectronic flip-flop, where the nonlinear characteristics of the VCSELs are utilized in a positive feedback scheme to achieve bistability.**

***Index Terms*—Optical interconnects, optoelectronic feedback, smart pixels, vertical cavity surface emitting lasers (VCSELs).**

I. Introduction

SMART pixel arrays (SPAs) are optoelectronic architectures, with a variety of applications in optically interconnected networks, smart sensors, and neural networks [1]–[3]. The interest in this field has intensified recently as the fundamental limitations of electronic interconnects are being approached [4], while at the same time, technological advancements have made the fabrication of larger and more complex SPAs more practical [5]–[7].

Usually SPAs consist of a set of individually addressable optical detectors and optical modulators or emitters. While the integration and fabrication of optical detectors and modulators is easier, the resulting architectures require additional expensive optics and external light sources. As a result, much attention is focused on emitter based SPAs, where the optical sources and detectors are fully integrated into the same array. Particularly attractive candidates for this purpose are SPAs incorporating vertical cavity surface emitting lasers (VCSEL) [8]. VCSELs are efficient sources of laser light, and they are particularly suitable for smart pixel applications because they can be fabricated conveniently in the form of two-dimensional (2-D) arrays with a perpendicular optical axis in the third dimension. Integration of light detectors such as metal-semiconductor-metal (MSM) detectors on the same substrate provides the necessary functionalities for the SPA to perform a variety of optoelectronic tasks, involving the receiving, processing, and transmission of optical and electrical signals in an inherently parallel manner.

Manuscript received October 15, 1999; revised July 21, 2000. This work was supported by the National Science Foundation under Grant ECS-9 871 479.

M. Azadeh and R. B. Darling are with the Department of Electrical Engineering, University of Washington, Seattle, WA 98195 USA..

W. R. Babbitt is with the Department of Physics, Montana State University, Bozeman, MT 59717 USA.

Publisher Item Identifier S 0733-8724(00)09104-0.

An in-depth analysis of SPAs is complicated by several factors. The individual pixels in a practical SPA usually are not totally isolated from each other. One of the inherent causes of this lack of isolation is the electrical and optical crosstalk between adjacent detectors and emitters. These devices are fabricated on the same chip and, therefore, share the same substrate. With shrinking dimensions and the interest in increasing the number of devices on a single chip, the devices may no longer be completely isolated, and various electrical leakage mechanisms may exist between adjacent pixels. The same factors result in additional complications for the emitters. While the ability to integrate relatively powerful VCSELs into arrays on a single chip is a definite advantage, the increased possibility of unwanted optical couplings between a VCSEL and the adjacent detectors is a side-effect to be considered. Therefore, in addition to electrical crosstalk, optical crosstalk between adjacent pixels has to be taken into consideration. Another complicating fact in the behavior of SPAs is the nonlinearity of light emitters, the most evident demonstrations of which are the threshold current and saturation in emitters. All these factors and their effects limit the dynamic range and the available space-bandwidth products for a given SPA, and must be understood and modeled as thoroughly as possible for SPAs to be used in their fullest capacity in information processing applications.

Cross-couplings between pixels within a SPA are not limited to crosstalk. There are numerous situations, in which the designer wants to take advantage of the on-chip processing capabilities of SPAs by introducing additional electronic or optical interconnections schemes within and between pixels to achieve improved performance or new functionalities. Such SPAs have applications in, among other areas, neural-networks, early vision processing, analog optoelectronics, and optoelectronic field-programmable gate arrays (OE-FPGA) [9]–[13]. Other problems addressable by such schemes are issues related to the nonlinearity and nonuniformity of optical sources. The most effective way to encounter these effects in semiconductor lasers is through the use of negative optoelectronic feedback. Feedback may also be used to achieve new functionalities, otherwise not commonly available [14], [15].

It is the aim of this paper to develop a formalism for modeling source-based SPAs, to include arbitrary optoelectronic interconnections as well as crosstalk and/or various feedback schemes within and between pixels in the presence of optical source nonlinearities. From a mathematical perspective, these schemes can be modeled using a single formalism, because they result in coupled equations for various variables within a single pixel or among various pixels within an array. Hence, the term "interconnection" in this paper is used in its general sense to mean

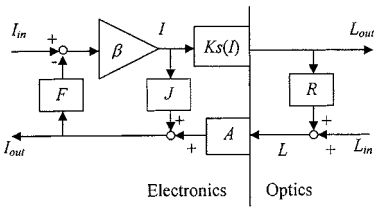

Fig. 1. Schematic diagram of a single smart pixel.

any electronic or optical coupling between the variables of one pixel or multiple pixels in a SPA. Models capable of accounting for such single- and multiple-pixel interactions are essential for better understanding the behavior of SPAs, and are crucial tools in the process of designing practical and new applications for such arrays.

Initially in this paper, the modeling of various interconnections and crosstalk mechanisms in the presence of source nonlinearity within a single pixel is addressed. Then the resulting concepts are generalized to multipixel interactions within an arbitrary SPA. The single pixel analysis presented in this paper is partly based on our previous work [16], with the difference that, in this research, we take a more general approach and concentrate on developing the concepts toward a multi-pixel array with nonlinear optical sources and arbitrary interconnectivity. As an experimental demonstration, we use optical feedback, positive electrical feedback, and the inherent nonlinearity of the VCSEL source to implement a VCSEL-based optoelectronic flip-flop.

II. Single-Pixel Analysis

In order to develop a general model for a SPA, it is useful to consider first a single pixel. Fig. 1 shows the schematic diagram of a single pixel, which consists of a light source, a detector, and driver and receiver circuits.

The pixel has an electronic input and an electronic output, $I_{\rm in}$ and $I_{\rm out}$. It also has an optical input and an optical output, $L_{\rm in}$ and $L_{\rm out}$. These optical signals refer to the intensity of the light. Further, it is assumed that the optical signals are mutually incoherent, so there are no interference effects present. The pixel can be thought of as an interface element, which allows for bi-directional exchange of electrical and optical signals. An important aspect of this model is that the optical source is modeled with a nonlinear function $Ks(I)$, where I is the output of the driver circuit β. This is important because, in general, all optical sources are nonlinear. They cannot produce a negative light if their input becomes negative, and usually they have a saturation current limiting the maximum output power of the pixel. Even within these two limits, the output may not be a linear function of the drive current. The same nonlinear function also may be used to model other nonlinearities in the system, such as power supply clipping of the signals or the nonlinearity in the gain of the driving circuit β. Therefore, all the nonlinearities are assumed to be lumped in the function $Ks(I)$. It should be noted that the same concerns are not generally applicable to the detector, because the optical input to the detector is always positive. Also the optical signal levels at the input of the detector are usually much lower than the pixel's optical output levels, which means it is usually sufficient to model the detector with a linear (possibly small signal) gain A.

In addition to the source and detector circuits, there may be several interconnection or crosstalk paths. There can exist optical feedback (or crosstalk), represented by R, from the output of the source to the detector's input. Another effect to be modeled is the current leakage from the source to the detector. This term is represented by J, and as shown later, can affect negatively the performance of the SPA. It should be noted that the opposite effect (current leakage from the detector to the emitter) is usually negligible, because the signal level at the output of the detector is usually very small compared to the emitter drive current I. We also allow for electronic feedback from the output of the detector to the input of the pixel. This feedback, denoted by F, is introduced intentionally usually to achieve closed loop behavior. For convenience and without any loss of generality, the output of the F block is subtracted from the electrical input, because usually F represents a negative feedback scheme to stabilize the output of the pixel. Later, we generalize F to model arbitrary electrical interconnection schemes between various pixels.

Ideally, when there are no electrical and/or optical crosstalk and also when no feedback is present ($F = J = R = 0$), the electrical and optical outputs of the pixel are given by:

$$I_{\rm out} = AL_{\rm in} \tag{1}$$

$$L_{\rm out} = Ks(\beta I_{\rm in}). \tag{2}$$

As mentioned earlier, however, the situation is usually more complicated in practical cases. The terms J and R may no longer be zero due to proximity of the detector and the source on the same substrate. Moreover, it may be useful to introduce intentionally additional on-chip processing capabilities or feedback schemes to achieve improved performance or specific functionalities. For example, as can be seen from (2), the optical output of the pixel depends on the form of the function Ks, which in general is nonlinear and depends on the characteristics of the individual device, with random variations from one device to the next. The most straightforward solution for these problems is to use negative feedback as represented by the F block.

In the general case, where F, J and R are nonzero, tracing of the signals around the loop results in the following implicit equation for $L_{\rm out}$:

$$L_{\rm out} = Ks\left(\frac{\beta}{1+FJ\beta}I_{\rm in} - \frac{FA\beta}{1+FJ\beta}L_{\rm in} - \frac{\beta FAR}{1+FJ\beta}L_{\rm out}\right). \tag{3}$$

Once $L_{\rm out}$ is found, other loop variables can also be found. A graphical solution to (3) provides insight into the behavior of the single pixel. Realizing that the argument of the Ks function is simply the drive current I, one can find the solution as the intersection of the function $L_{\rm out} = Ks(I)$ and a load line given by

$$L_{\rm out} = -\frac{1+FJ\beta}{FAR\beta}I + \frac{1}{FAR}I_{\rm in} - \frac{1}{R}L_{\rm in}. \tag{4}$$

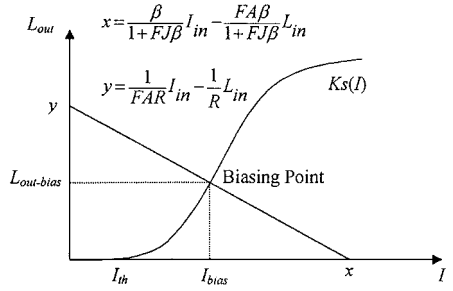

Fig. 2. Graphical solution for a single pixel.

Fig. 2 illustrates this situation for a typical $Ks(I)$ function, with a threshold and saturation behavior. The intersection of the load line with each axis is also shown in the figure. It is realized that, in order for the loop to be biased in the active region with a single solution (the situation implicitly assumed in the figure), a necessary condition is that *both* these relations hold

$$\frac{1}{FA}I_{\mathrm{in}} > L_{\mathrm{in}} \tag{5}$$

$$I_{\mathrm{in}} - FAL_{\mathrm{in}} > \frac{1+FJ\beta}{\beta}I_{\mathrm{th}}. \tag{6}$$

Equation (5) requires negative feedback (positive F) while (6) limits L_{in} for a given I_{in} and I_{th}. If, on the other hand, a multistable or digital on-off behavior is needed, (5) and/or (6) can be violated and the desired behavior can be achieved by proper choice of the loop parameters. For example, the bistable behavior in the optoelectronic flip-flop discussed at the end of this paper is achieved by violation of these inequalities. A case of special interest for analog applications is to use negative feedback to make the output of the pixel independent of the device characteristics. Usually, this is achieved by increasing the loop gain β and making it large ($\beta \to \infty$) in which case the load line in Fig. 2 tends to become horizontal. If the current leakage is negligible ($J = 0$) the optical output is given by

$$L_{\mathrm{out}} = \frac{1}{FAR}I_{\mathrm{in}} - \frac{1}{R}L_{\mathrm{in}}. \tag{7}$$

The importance of this case is that the optical output is independent of the function $Ks(I)$, and is linearized in both I_{in} and L_{in}. At the same time, this underlines the importance of having negligible leakage current levels because (7) holds only when $J = 0$. Therefore, it can be deduced that in general the leakage current deteriorates the performance of a negative feedback loop.

III. Multipixel Analysis

The case of a single pixel discussed in Section II can be used as a basis for analyzing the behavior of a SPA with arbitrary interconnectivity. In the following analysis, we add an index i to all the signal quantities referring to an arbitrary ith pixel within the array. On the other hand, the interconnections are shown with double indexes. For example, J_{ii} and J_{ij} represent the internal emitter-detector current leakage for pixel i, and the current leakage from the emitter of pixel j to the detector of pixel i, respectively. We also adopt the summation over repeated index convention, so the repeated index is a dummy index summed

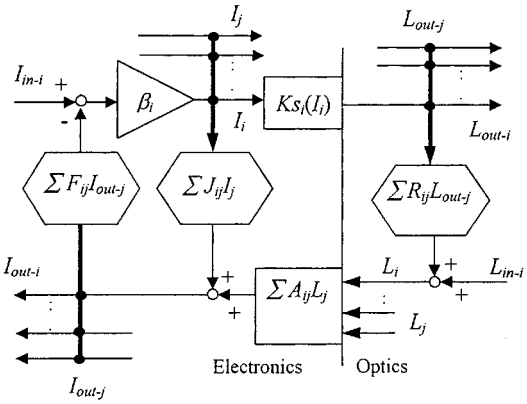

Fig. 3. Schematic diagram of a fully interconnected SPA.

over all the pixels within the array. Fig. 3 shows the schematic diagram of an arbitrary interconnected SPA following this notation.

In this figure $\mathbf{F} = [F_{ij}]$ and $\mathbf{R} = [R_{ij}]$ represent the electrical and optical interconnectivity matrices. These matrices model individual electrical and optical gains within pixels and cross-couplings between various pixels. The two matrices $\mathbf{A} = [A_{ij}]$ and $\mathbf{J} = [J_{ij}]$ are the detector crosstalk and current leakage matrices, respectively. The matrix $\beta = [\beta_i]$ is a diagonal matrix with elements β_i. By choosing β to be diagonal, we have assumed implicitly that there is no cross-coupling between the drivers of the various pixels. This is a reasonable assumption because usually driver circuits operate on high current levels, nevertheless, generalization to a nondiagonal β is straightforward. The signal quantities are represented by $\mathbf{I_{in}} = [I_{\mathrm{in}-i}], \mathbf{L_{in}} = [L_{\mathrm{in}-i}]$ and $\mathbf{L_{out}} = [L_{\mathrm{out}-i}]$; the electrical input, the optical input, and the optical output vectors, respectively. Here $\mathbf{F}, \mathbf{A}, \mathbf{J}, \beta$, and $\mathbf{R}$ are square $n \times n$ matrices, and $\mathbf{I_{in}}, \mathbf{L_{in}}$, and $\mathbf{L_{out}}$ are $n \times 1$ vectors, where n is the total number of pixels.

To analyze the array, we notice that

$$I_i = \beta_i \left[I_{\mathrm{in}-i} - \sum F_{ij} I_{\mathrm{out}-j} \right] \tag{8}$$

while $I_{\mathrm{out}-j}$ can itself be written as

$$I_{\mathrm{out}-j} = \sum A_{jk} L_k + \sum J_{jk} I_k \tag{9}$$

and L_k can be written as

$$L_k = L_{\mathrm{in}-k} + \sum R_{kn} L_{\mathrm{out}-n}, \tag{10}$$

Combining (9), (10), and (8) and noticing the repeated indexes are dummy indexes to be summed over, we find

$$\mathbf{I} = \beta[\mathbf{I_{in}} - \mathbf{FJI} - \mathbf{FAL_{in}} - \mathbf{FARL_{out}}]. \tag{11}$$

Solving (11) for $\mathbf{I}$ results:

$$\mathbf{I} = [\mathbf{I_e} + \beta\mathbf{FJ}]^{-1}\beta[\mathbf{I_{in}} - \mathbf{FAL_{in}} - \mathbf{FARL_{out}}] \tag{12}$$

where $\mathbf{I_e}$ is the square $n \times n$ identity matrix and it is assumed that $\mathbf{I_e} + \beta\mathbf{FJ}$ is a nonsingular and hence invertible matrix. It should

be noticed that a sufficient condition for the nonsingularity of this matrix is $\mathbf{J} = \mathbf{0}$.

If we define the vector notation

$$\mathbf{L_{out}} = \mathbf{Ks}[\mathbf{I}] \equiv [Ks_i(I_i)], \tag{13}$$

a formal solution for the array can be obtained

$$\mathbf{L_{out}} = \mathbf{Ks}([\mathbf{I_e} + \beta\mathbf{FJ}]^{-1}\beta[\mathbf{I_{in}} - \mathbf{FAL_{in}} - \mathbf{FARL_{out}}]). \tag{14}$$

Therefore, (14) can be considered as the matrix generalization of (3). For instance, an obvious special case is when the matrices $\mathbf{F}, \mathbf{A}, \mathbf{J}$, and $\mathbf{R}$ are diagonal (no pixel-pixel interaction). Then (14) decouples into separate equations of the from given by (3). While (14) is an implicit equation in terms of $\mathbf{L_{out}}$, it is also possible to obtain an equivalent set in terms of the variable $\mathbf{I}$ by substituting (13) directly into (11)

$$\mathbf{I} = \beta[\mathbf{I_{in}} + \mathbf{FJI} + \mathbf{FAL_{in}} + \mathbf{FARKs}[\mathbf{I}]]. \tag{15}$$

The advantage of (15) over (14) is that there are no matrix inversions involved.

Although, in general, (14) or (15) have to be solved numerically, for example by self-iterative methods, there are special cases where closed form analytical solutions may be found. As examples of such cases, we discuss two important special cases, (a) strong negative feedback and (b) a linear source.

A. Strong Negative Feedback Solution

It is often desired to implement negative feedback to stabilize and linearize the output of nonlinear sources such as semiconductor lasers. For SPAs, this can be achieved by increasing the individual loop gains ($\beta_i \to \infty$ for all i) within the negative feedback loops. For simplicity, we assume the current leakage is negligible ($\mathbf{J} = \mathbf{0}$). In this case, (12) reduces to

$$\mathbf{I} = \beta[\mathbf{I_{in}} - \mathbf{FAL_{in}} - \mathbf{FARL_{out}}] \tag{16}$$

Because β is a diagonal matrix with nonzero elements, it is invertible, and (16) can be written as

$$\beta^{-1}\mathbf{I} = \mathbf{I_{in}} - \mathbf{FAL_{in}} - \mathbf{FARL_{out}} \tag{17}$$

For the case of high loop gains ($\beta_i \to \infty$ for all i) the left hand side of (17) is a vector with small elements ($\beta^{-1}\mathbf{I} \cong \mathbf{0}$) and therefore we obtain

$$\mathbf{L_{out}} = [\mathbf{FAR}]^{-1}\mathbf{I_{in}} - \mathbf{R}^{-1}\mathbf{L_{in}}. \tag{18}$$

This equation is clearly the generalized form of (7) for the single pixel. The importance of this solution, just like the case of a single pixel, is that the optical output vector of the array is expressed as the sum of two linear transformations of the optical and electrical input vectors. This solution also has interesting implications in optical computing applications, because it can be used to implement the operations of matrix-vector and matrix-matrix multiplication as well as matrix inversion.

B. Linear Source Solution

Another important especial case, in which closed loop solutions may be found, is when the optical emitters can be modeled with a threshold current $I_{\rm th}$ and a linear gain K above threshold, so for the ith emitter

$$L_{{\rm out}-i}(I_i) = \begin{cases} 0 & I_i < I_{{\rm th}-i} \\ K_i(I_i - I_{{\rm th}-i}) & I_i > I_{{\rm th}-i} \end{cases}. \tag{19}$$

This model is particularly useful for VCSELs, because they have a threshold current below which their optical output is small, and above it the optical output increases relatively linearly with drive current. The linear solution is also useful in small signal analysis, where the whole system is linearized around some operating point.

Using the matrix notation introduced in (13), and assuming all emitters are biased above threshold, (19) can be written as

$$\mathbf{L_{out}}(\mathbf{I}) = \mathbf{K}(\mathbf{I} - \mathbf{I_{th}}) \tag{20}$$

where $\mathbf{K}$ is a square diagonal matrix with elements K_i and $\mathbf{I_{th}}$ is a vector with elements $I_{{\rm th}-i}$. If (20) is substituted into (11), a closed-form solution is obtained

$$\mathbf{I} = \mathbf{M}^{-1}\mathbf{I_{in}} + \mathbf{M}^{-1}\mathbf{FAL_{in}} - \mathbf{M}^{-1}\mathbf{FARKI_{th}} \tag{21}$$

where

$$\mathbf{M} = \beta^{-1} - \mathbf{FJ} - \mathbf{FARK}. \tag{22}$$

The optical output vector $\mathbf{L_{out}}$ is obtained easily from (21) and (20). The validity of this solution is limited to the case where the array is biased in the active region, a necessary condition for which is that $\mathbf{M}$ should be nonsingular. If $\mathbf{M}$ becomes close to singular, some elements of $\mathbf{I}$ may become very large or negative, and this contradicts our assumption of active biasing. In this case, the solution given by (21) is invalid, and the general nonlinear (14) or (15) should be used.

IV. Experimental Demonstration: An Optoelectronic Flip-Flop

As an experimental verification of some of the models discussed in this paper, we demonstrate the application of these models in the analysis and design of a VCSEL-based optoelectronic flip-flop. In Section II, we discussed the concept of a load-line generated by the feedback loop around a nonlinear optical source. In this experimental demonstration, we use the inherent nonlinearity in the VCSELs to create bistability. The bistable behavior of the pixel can be used then to make an optoelectronic flip-flop.

The underlying principle of such a flip-flop is illustrated in Fig. 4, which is essentially a special case of Fig. 2. The difference here is that the form of the nonlinearity is chosen to represent a VCSEL with the threshold current and threshold output $I_{\rm th}$ and $L_{\rm th}$, and the saturation current and saturation output $I_{\rm sat}$ and $L_{\rm sat}$. The saturation can be intrinsic to the device, or be made to represent current limiting due to driver circuits. Also, three instances of the load-line, d_1, d, and d_2 with horizontal axis intersections x_1, x, and x_2, are shown

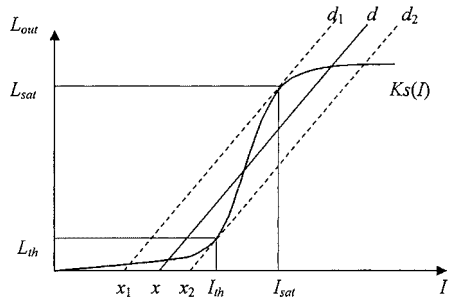

Fig. 4. Graphical illustration of the use of VCSEL nonlinearity and positive feedback to implement an optoelectronic flip-flop.

for a positive feedback (negative F) case. The variable x is a function of loop parameters and the optical and electrical inputs $L_{\rm in}$ and $I_{\rm in}$

$$x = \frac{\beta}{1+FJ\beta} I_{\rm in} - \frac{FA\beta}{1+FJ\beta} L_{\rm in} \tag{23}$$

and the slope of the load-line is given by

$$m = -\frac{1+FJ\beta}{FAR\beta}. \tag{24}$$

It can be seen that, as the inputs to the pixel, $L_{\rm in}$ and $I_{\rm in}$, vary, the load-line shifts left or right, while its slope remains constant. As the load-line moves from left to right, the VCSEL is biased first below threshold, and as the load-line passes d_2, the VCSEL is switched on to saturation. On the other hand, if the load-line moves toward the left, the VCSEL is biased initially in the saturation region, and as the load-line passes d_1, it is switched off to sub-threshold. Therefore, hysteresis is created, which can be utilized to implement an optoelectronic flip-flop. It should be noted that, while the load-line is between d_2 and d_1, a third solution (in the active region) is mathematically possible. However, this is an unstable solution because of the positive feedback loop.

Using (23) and (24), and for a given VCSEL characteristic, the pixel's parameters are chosen, so that the load-line is normally located between d_1 and d_2. Once an input optical pulse $L_{\rm in}$ is received, the load-line moves to the right of d_2. When the optical pulse is removed, the load-line returns to its normal position, but the pixel stays on. This constitutes the "set" operation of the flip-flop. To turn off the pixel, a negative pulse on the biasing input current $I_{\rm in}$ should be applied. Decreasing $I_{\rm in}$ causes the load-line to move left passed d_1, resulting in flipping the VCSEL to sub-threshold biasing. Now, if the negative pulse on $I_{\rm in}$ is removed, the load-line again returns to its normal position between d_1 and d_2, but the pixel stays off. This constitutes the "reset" operation of the flip-flop.

For an experimental demonstration, we used a 4×4 array of VCSELs interlaced with a 4×4 array of MSM detectors. The photograph of a sample VCSEL in this array, surrounded by 4 MSM neighboring detectors, is shown in Fig. 5, and the output characteristic of it is shown in Fig. 6. Using CMOS driver circuits, the saturation current and output were limited to roughly 11.5 mA and 95 μW, respectively. The current leakage coefficient between the VCSEL and the adjacent MSM detector

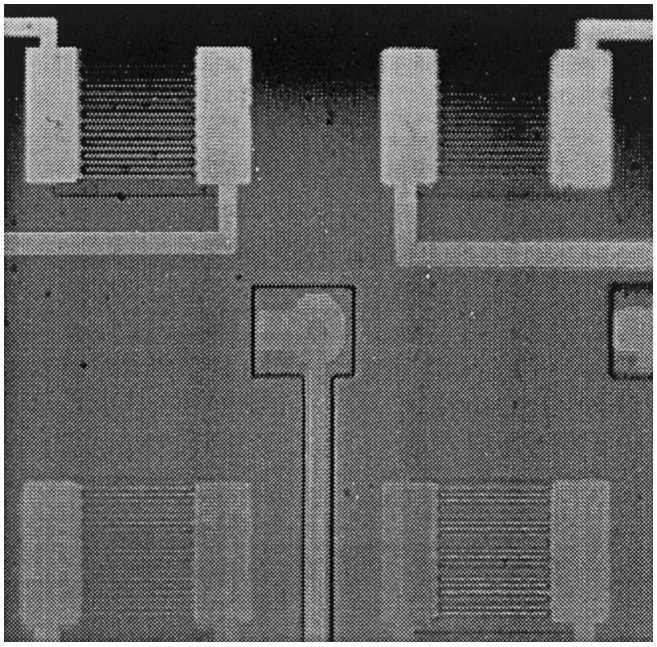

Fig. 5. Photograph of a sample VCSEL of the array surrounded by 4 MSM detectors.

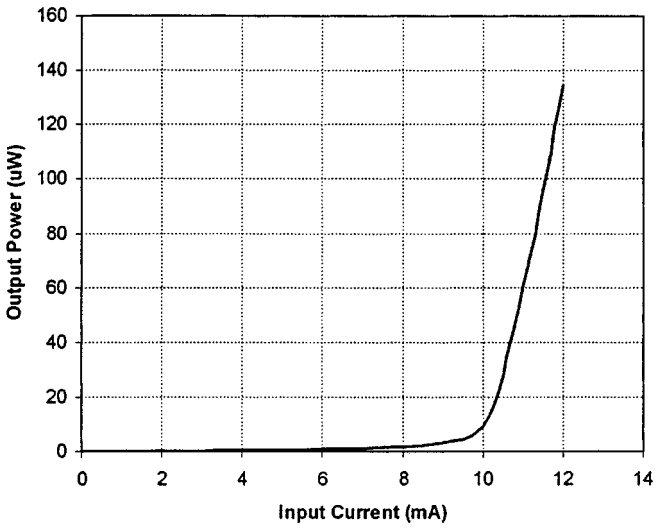

Fig. 6. Output characteristic of the VCSEL used in the experiments.

was measured to be $J = 2.7 \times 10^{-5}$. The gain of the detector was $A = 0.3$ A/W, and the electrical loop-gain was set at $FA\beta = -0.79$ mA/μW. The optical feedback coefficient was set to $R = 0.09$. The leakage loop gain was $FJ\beta = -0.071$, much smaller than unity. This meant that the effect of the leakage current was small. These parameters resulted in a load-line slope of $m = 13\,\mu$W/mA according to (24). The slope of the VCSEL characteristic in the active region was roughly 43 μW/mA, larger than the slope of the load-line. This ensured that the situation depicted in Fig. 4 was realizable.

Using an external laser source, an optical input was applied to the pixel and gradually increased, while the optical output of the pixel was being monitored. A plot of the optical output versus the optical input is given in Fig. 7. As the optical input

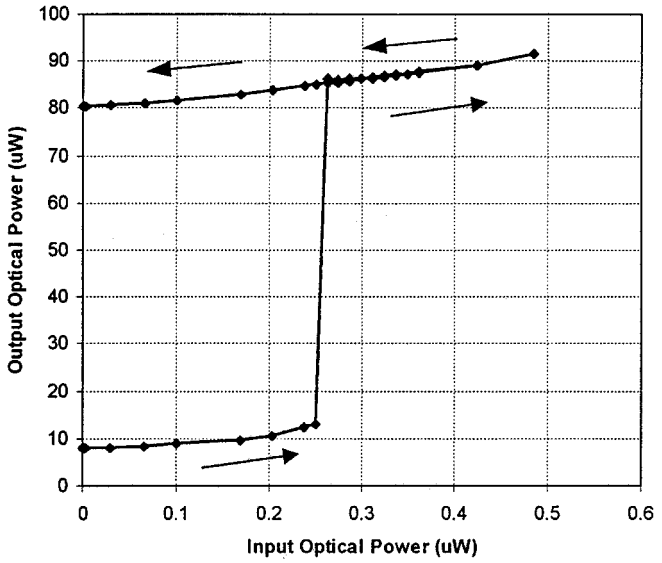

Fig. 7. Demonstration of input optical pulse capture.

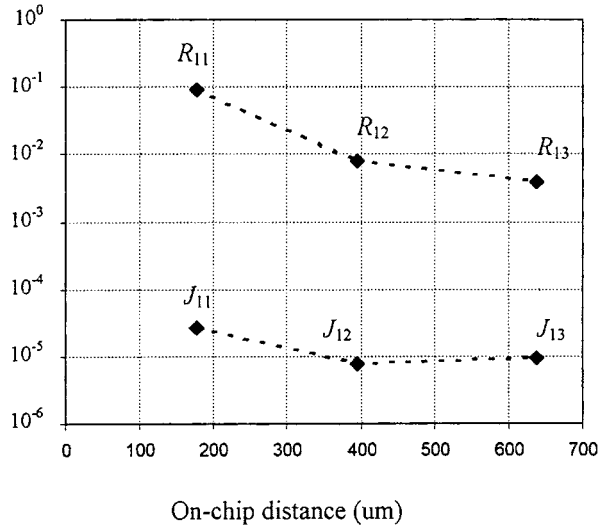

Fig. 8. Optical feedback and current leakage coefficients $(R_{11}, R_{12}, R_{13}, J_{11}, J_{12}, J_{13})$ for three VCSEL sources versus on-chip distance.

was increased, the optical output of the VCSEL also increased. This corresponds to moving the load-line with the slope of $m = 13\,\mu$W/mA in the sub-threshold region of the VCSEL characteristic resulting in sub-threshold output powers. From Fig. 7, it is seen that the pixel flips on at an optical input power of about 0.25 μW. At this point the output power is about 13 μW, in agreement with the threshold output of the VCSEL seen in Fig. 6. Once the VCSEL is flipped on, the output is limited by the driver circuits. The slope of the curve in this region corresponds to the output impedance of the driver circuits. The optical input then was reduced, causing the VCSELs output to also reduce. Nevertheless, the pixel stayed on, even when the optical input signal was reduced down to zero. This demonstrates the capture of an optical input pulse by the flip-flop. To "reset" the flip-flop, the electrical input I_{in}, which biases the loop should be decreased, as previously explained.

The operation of the flip-flop discussed so far is based on a single pixel analysis. To demonstrate multi-pixel effects, we now address crosstalk mechanisms between adjacent pixels. First, we measure the optical interconnection and current leakage coefficients (R_{ij} and J_{ij}) from VCSEL sources further away on the chip. The quantities, related to the flip-flop, are denoted by index 1, and the adjacent VCSELs are denoted by higher indexes. This measurement can be done by turning on the adjacent VCSELs and measuring the output of the detector. The results of these measurements for VCSEL-1, as well as two additional VCSEL sources, are: $J_{11} = 2.7 \times 10^{-5}, J_{12} = 7.8 \times 10^{-6}, J_{13} = 9.4 \times 10^{-6}, R_{11} = 0.9, R_{12} = 0.008$, and $R_{13} = 0.004$. These results are also shown in Fig. 8. It should be noticed that the R_{11} and J_{11} coefficients are the same as the R and J coefficients of the flip-flop. The measured coefficients are plotted against the distance from the centers of VCSELs to center of detector. It can be seen that the optical interconnection coefficient reduces almost one order of magnitude by going from the closest VCSEL to the next VCSEL further away. This is expected because the first VCSEL was coupled intentionally to the detector to implement optical feedback. However, the

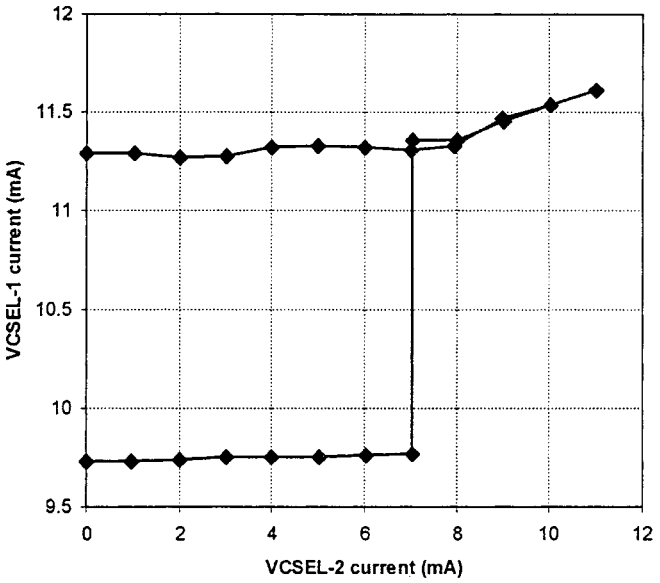

Fig. 9. Demonstration of crosstalk effect from a second VCSEL source on the flip-flop.

couplings from VCSELs further away can be attributed to stray light and inaccuracies in the optical system. The current leakage coefficient also decreases by going from the adjacent VCSEL to the next VCSEL, however, it slightly increases for the third VCSEL. This anomalous behavior was verified several times in different experiments, and may be due to the underlying geometry of the various layers on the chip. The determination of the exact cause(s) of this behavior lies outside the scope of this paper, and needs further investigation.

The effects of the adjacent sources on the behavior of the flip-flop can be modeled using the multi-pixel analysis of Section III. For simplicity, we focus only on the effects of couplings with a single additional VCSEL. In this case, the operating point of the adjacent pixel can be set independently, because there is

no electrical interconnection present ($F_{22} = F_{12} = F_{21} = 0$). However, the operating point of the extra VCSEL affects the load-line of the pixel implementing the flip-flop. In fact, if we write the first component of (12), and solve for the optical output of the first pixel (flip-flop), we obtain a load line in the form

$$L_{\text{out}-1} = -\frac{1+\beta_{11}F_{11}J_{11}}{\beta_{11}F_{11}A_{11}R_{11}}I_1 + \frac{1}{F_{11}A_{11}R_{11}}I_{\text{in}-1} - \frac{J_{12}}{A_{11}R_{11}}I_2 - \frac{R_{12}}{R_{11}}L_{\text{out}-2}. \quad (25)$$

Equation (25) predicts that the drive current and the optical output of the second VCSEL can shift the load-line of the first pixel to left or right without affecting its slope. It can be verified from (25) that, if F_{11} is negative (positive feedback for first pixel), increasing I_2 and $L_{\text{out}-2}$ shifts the load-line to the right, causing the flip-flop to turn on. This was observed experimentally, and the results are shown in Fig. 9. In this figure, the drive-current of the adjacent VCSEL was swept, while the drive-current of the first VCSEL (corresponding to the flip-flop) was being observed. The flip-flop switched on, when the driving current of the second VCSEL exceeded 7 mA, which roughly coincided with its threshold current. Moreover, the slope of the curve after switch-on is significantly higher compared to when the flip-flop is off (where the slope is nearly zero). This means that, in this case, the main contribution to crosstalk from the adjacent VCSEL to the flip-flop is optical for two nearest neighbor VCSELs. For VCSELs further apart, the optical couplings may decrease to a leve, in which optical and electrical couplings become comparable.

V. Conclusion

We have developed theoretical models of smart pixels and their individual performance, as well as their performance in conjunction with other pixels in a fully interconnected SPA. These models are crucial tools for the analysis and development of new applications for SPAs, especially as the number of devices per area on a single chip continues to rise, while the trend to take advantage of parallel on-chip processing and full optoelectronic interconnectivity capabilities of SPAs is becoming more important. The models include the nonlinearities in the emitters, as well as various leakage, cross-couplings, and more general optical and electrical interconnections between the pixels. Closed form solutions for two important special cases were obtained. As an experimental verification of the developed models, we have demonstrated the application of the theory in the design and implementation of a VCSEL-based smart pixel optoelectronic flip-flop.

Acknowledgment

The authors would like to thank the Consortium for Optical and Optoelectronic Technologies in Computing (CO-OP) for providing the VCSEL array used in the experiments.

References

[1] D. S. Wills, J. M. Baker, H. H. Cat, S. M. Chai, L. Codrescu, J. Cruz-Rivera, J. C. Eble, A. Gentile, M. A. Hopper, W. S. Lacy, A. Lopez-Lagunas, P. May, S. Smith, and T. Taha, "Processing architectures for smart pixel systems," *IEEE J. Select. Topics Quantum Electron.*, vol. 2, pp. 24–33, Apr. 1996.

[2] D. S. Kim, J. C. Dries, M. R. Gokhale, and S. R. Forrest, "Optoelectronic InP-InGaAs smart pixels for optical interconnections and computing," *IEEE J. Quantum Electron.*, vol. 33, pp. 1407–1416, Aug. 1997.

[3] D. Bartzos, P. Panayotatos, S. R. McAfee, and D. G. Daut, "Parameter extraction for a figure-of-merit approach for the comparison of optical interconnects," *Opt. Eng.*, vol. 37, no. 10, pp. 2772–2783, Oct. 1998.

[4] D. A. B. Miller, "Physical reasons for optical interconnects," *Int. J. Optoelectron.*, vol. 11, pp. 155–168, 1997.

[5] J. F. Ahadian and C. G. Fonstad, "The epitaxy-on-electronics technology for monolithic optoelectronic integration: Foundations, development, and status," *Opt. Eng.*, vol. 37, pp. 3161–3174, Dec. 1998.

[6] J. F. Ahadian, P. T. Vaidyanathan, S. G. Patterson, Y. Royter, D. Mull, G. S. Petrich, W. D. Goodhue, S. Prasad, L. A. Kolodziejski, and C. G. Fonstad, "Practical OEIC's based on the monolithic integration of GaAs-InGaP LED's with commercial GaAs VLSI electronics," *IEEE J. Quantum Electron.*, vol. 34, pp. 1117–1123, July 1998.

[7] H. Kosaka, "Smart integration and packaging of 2-D VCSEL's for high-speed parallel links," *IEEE J. Select. Topics Quantum Electron.*, vol. 5, no. 2, pp. 184–192, Mar./Apr. 1999.

[8] W. W. Chow, K. D. Choquette, M. H. Crawford, L. K. Lear, and G. R. Hadley, "Design, fabrication, and performance of infrared and visible vertical-cavity surface-emitting lasers," *IEEE J. Quantum Electron.*, vol. 33, pp. 1810–1824, Oct. 1997.

[9] T. G. Morris and S. P. DeWeerth, "Analogue VLSI morphological image processing circuit," *Electron. Lett.*, vol. 31, pp. 1998–1999, Nov. 1995.

[10] M. H. Brill, D. W. Bergeron, and W. W. Stonet, "Retinal model with adaptive contrast sensitivity and resolution," *Appl. Opt.*, vol. 26, pp. 4993–4998, Dec. 1987.

[11] H. Ikeda, K. Tsuji, T. Asai, H. Yonezu, and J. Shin, "A novel retina chip with simple wiring for edge extraction," *IEEE Photon. Technol. Lett.*, vol. 10, no. 2, pp. 261–263, Feb. 1998.

[12] Y. Joo, J. Park, M. Thomas, K. S. Chung, M. A. Brooke, N. M. Jokerst, and D. S. Wills, "Smart CMOS focal plane arrays: A Si CMOS detector array and sigma-delta analog-to-digital converter imaging system," *IEEE J. Select. Topics Quantum Electron.*, vol. 5, no. 2, pp. 296–305, Mar./Apr. 1999.

[13] J. V. Campenhout, H. V. Mark, J. Depreitere, and J. Dambre, "Optoelectronic FPGA's," *IEEE J. Select. Topics Quantum Electron.*, vol. 5, no. 2, pp. 306–315, Mar./Apr. 1999.

[14] J. S. Kane, T. G. Kincaid, and P. Hemmer, "Optical processing with feedback using smart pixel spatial light modulators," *Opt. Eng.*, vol. 37, no. 3, pp. 942–947, Mar. 1998.

[15] M. Azadeh, W. R. Babbitt, and R. B. Darling, "Smart pixels with smart illumination," *Opt. Lett.*, vol. 23, no. 10, pp. 786–788, May 1998.

[16] M. Azadeh, R. B. Darling, and W. R. Babbitt, "Characteristics of optoelectronic feedback for smart pixels with smart illumination," *IEEE J. Select. Topics Quantum Electron.*, vol. 5, no. 2, pp. 172–177, Mar./Apr. 1999.

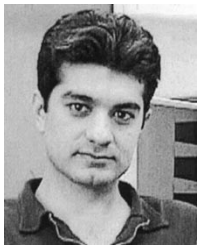

Mohammad Azadeh was born in Tehran, Iran, on June 4, 1965. He received the B.S. degree in electrical engineering from Tehran University in 1988, his M.S.E.E. from Portland State University in 1995, and the Ph.D. degree from University of Washington in 2000.

His research interests include mixed signal VLSI, optoelectronics, and microfabrication.

Robert B. Darling (S'78–M'86–SM'94) was born in Johnson City, TN, on March 15, 1958. He received the B.S.E.E. (with highest honors), M.S.E.E., and Ph.D. degrees in electrical engineering from the Georgia Institute of Technology, Atlanta. in 1980, 1982, and 1985, respectively.

He has held summer positions with Sperry-Univac, Bristol, TN, Texas Instruments, Johnson City, TN, and from 1982 to 1983, he was with the Physical Sciences Division of the Georgia Tech Research Institute, Atlanta, GA. Since 1985, he has been with the Department of Electrical Engineering, University of Washington, Seattle, where he is presently an Associate Professor. From 1995 to 1996, he was a Visiting Associate Professor at Stanford University, Stanford, CA. His research interests include electron device physics, device modeling, microfabrication, circuit design, optoelectronics, sensors, electrochemistry, and instrumentation electronics.

Dr. Darling is a member of the American Physical Society, the American Vacuum Society, the Optical Society of America (OSA), and the American Association for the Advancement of Science.

W. Randall Babbitt was born in Pittsburgh, PA, on July 17, 1960. He received the B.S. degree in physics with honors and distinction from Stanford University, CA, in 1982 and the M.A. and Ph.D. degrees in physics from Harvard University, Cambridge, MA, in 1986 and 1987, respectively.

He was a Research Scientist at the Boeing High Technology Center from 1987 to 1993. He was a Research Assistant Professor and Research Associate Professor of Electrical Engineering at the University of Washington from 1993 to 1997 and continues his association with the department as an Affiliate Associate Professor of Electrical Engineering. In 1997, he joined Montana State University, Bozeman, as an Associate Professor of Physics. His research interests include optical processing, delay, and memory, spectral-spatial holography, optoelectronic image sensors, and optical and atomic physics.

Dr. Babbitt is a member of the American Physical Society and the Optical Society of America (OSA).